ISEF 2005 - XII International Symposium on Electromagnetic Fields
in Mechatronics, Electrical and Electronic Engineering
Baiona, Spain, September 15-17, 2005

Verification of axi-periodic analysis with 3D-FEA and calculation of eddy current loss of flux shield in the large turbo generator using axi-periodic analysis

S. O. Kwon, Hyuk Nam, B. Y. Choi, J. P. Hong, *Senior Member, IEEE*

Dept. Electrical Eng., Changwon Nat'l Univ., Changwon. Gyeongnam, 641-773 Korea
LG Electronics.
Doosanheavy Industires and Construction Co., Ltd.
(kso1975@changwon.ac.kr)

Abstract –Axi-periodic analysis for end region of large turbine generator is studied and verified by 3D-FEA in this paper. Verification is done by comparing three components of flux densities from axi-periodic analysis and 3D FEA in static field, and the comparison shows some differences, and the cause of those differences are studied. Even though, the differences, considering computation time and effort for modeling of 3D FEA, the errors would be acceptable for initial design of large turbine generator. Then, axi-periodic analysis is extended to time harmonic field for its application. From the time harmonic field analysis, the effect of flux shield and eddy current loss in the flux shield for power angles are presented.

Introduction

As a quasi 3-dimensional analysis, axi-periodic analysis is applied to the magnetic field for the end region of large turbine generator in [1] - [6]. Since axi-periodic analysis provides 3-dimensional flux distributions with 2-dimensional finite element modeling, it reduces computation time and efforts greatly comparing to 3D FEA. Many researches, applications, and verifications for axi-periodic analysis have been done since 1970's. However, the verifications are made only by measurements in small regions because measurements of flux density in the end region are limited in practical aspects.

Therefore, axi-periodic analysis is verified by 3D-FEA in this paper. Three components of flux densities from axi-periodic analysis and 3D FEA are compared in static field. To do that, 3D FEA model is constructed precisely including stator end windings based on an actual large turbine generator.

Axi-periodic formulations for time harmonic field using magnetic vector potential is firstly set for the field analysis. Then, three components of flux densitis from axi-periodic analysis are compared to that from 3D FEA in the static field. The comparison shows differences, and the cause of the error is studied. In spite of the differences, considering computation time and effort for modeling of 3D FEA, the errors would be acceptable for initial design of large turbine generator.

Axi-periodic analysis is extended to time harmonic field for its application. In time harmonic field analysis, eddy current loss in flux shield for load condition is calculated, and flux distribution due to the eddy current in flux shield is presented.

In the large turbine generator (ratings of 500MW or over), leakage flux in the stator end windings is the major design limitation of capacity due to the thermal effect caused by eddy current in stator end [1], [2]. The eddy current on the stator end region is mainly produced by axial component of leakage flux of stator and rotor end windings, and to prevent the axial flux impinging to the stator end, the flux shield made of copper is placed in the stator end region of large turbine generator. Due to the eddy current on the flux shield, leakage flux cannot go through the stator end region, and temperature in the flux shield can be high. However, flux shield is made of copper having high thermal conductivity, therefore, cooling can be easy comparing laminated stator core.

Analysis theory

In order to apply the finite element method to an axi-periodic model, following assumptions are made:[3]

a) Slot effects are not considered
b) Displacement current is ignored.
c) Magnetic material is isotropic with infinite permeability.
d) The analysis model is axi-symmetric.
e) Current density in rotor and stator windings are assumed to be consist of axial and circumferential components with sinusoidal distributions along axial and circumferential direction respectively.

Governing equations using vector potential for time harmonic fields are (1) and (2).

$$\nabla \times (\nu \nabla \times \vec{A}) = -\sigma(\frac{\partial \vec{A}}{\partial t} + \nabla \phi) + \vec{J}_o \tag{1}$$

$$\nabla \cdot (\sigma \frac{\partial \vec{A}}{\partial t} + \sigma \nabla \phi) = 0 \tag{2}$$

where, ν, $\vec{A}$, σ, ϕ, and $\vec{J}_o$ is magnetic reluctivity, magnetic vector potential, conductivity, electric scalar potential, and current density respectively.

Weighting function (W_i) and shape function (N_i) for Galerkin formulation are (3) and (4) respectively, and residuals are represented in (5) and (6).

$$W_i = N_i(r,z)e^{jp\theta} \tag{3}$$

$$N_i(r,\theta,z) = N_i(r,z)e^{-jp\theta} \tag{4}$$

$$R = -\int \nabla(N_i e^{jp\theta}) \times (\nu \nabla \times \vec{A}) dv + j\omega\sigma \int (N_i e^{jp\theta})\vec{A} dv + \sigma \int (N_i e^{jp\theta}) \nabla \phi dv - \int (N_i e^{jp\theta}) \vec{J}_o dv \tag{5}$$

$$R_\phi = -\int \nabla(N_i e^{jp\theta}) \cdot (j\omega\sigma \vec{A} + \sigma \nabla \phi) dv \tag{6}$$

Using N_i, magnetic vector potentials and electric scalar potentials are represented in r-z plane by (7) – (10).

$$A_r(r,\theta,z) = \sum_k A_r^{\,k} N_k(r,z)e^{-jp\theta} \tag{7}$$

$$A_\theta(r,\theta,z) = \sum_k A_\theta^{\,k} N_k(r,z)e^{-jp\theta} \tag{8}$$

$$A_z(r,\theta,z) = \sum_k A_z^{\,k} N_k(r,z)e^{-jp\theta} \tag{9}$$

$$\phi(r,\theta,z) = \sum_k \phi_k N_k(r,z)e^{-jp\theta} \tag{10}$$

Current distributions in conductors are represented by (11) - (13).

$$J_{or}(r,\theta,z) = J_r(r,z)e^{-jp\theta} \tag{11}$$

$$J_{o\theta}(r,\theta,z) = J_\theta(r,z)e^{-jp\theta} \tag{12}$$

$$J_{oz}(r,\theta,z) = J_z(r,z)e^{-jp\theta} \tag{13}$$

Analysis model

3D analysis model of 800MW turbine generator is shown in Fig. 3. Based on the periodicity and symmetry, 1/4 model is used for 3D FEA. Commercial software, Flux-3D, is used and analysis is performed in magneto static field. Field variable of 3D FEA is magnetic scalar potential; armature windings are modeled with non-meshed coils. 3D FEA model is precisely constructed considering stepped core and end step of stator as well as stator end windings, but non-magnetic retaining ring of rotor and flange of stator core are not considered. For stator end windings, coordinates of the windings are obtained from actual generator and one top and bottom coils consist of 10 segments of coils. 420,000 of elements are used and it takes 5 hours for single step with Pentium IV and 2GB RAM.

Axi-periodic analysis model is shown in Fig. 2, non-magnetic flange is not considered in the analysis and modeled region represents when a-phase is peaking. To make the comparison easy, only stator windings are excited for both analysis models. Fundamental component of current is applied to the stator and rotor end windings for the analysis. Total number of elements is 14,000, and it takes about 30 seconds for single step.

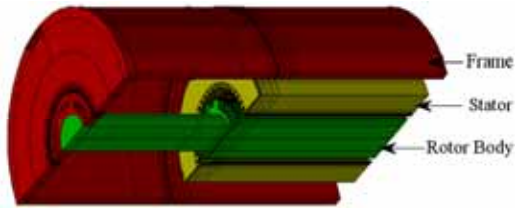

(a) Cross section of large turbine generator (1/4 model)

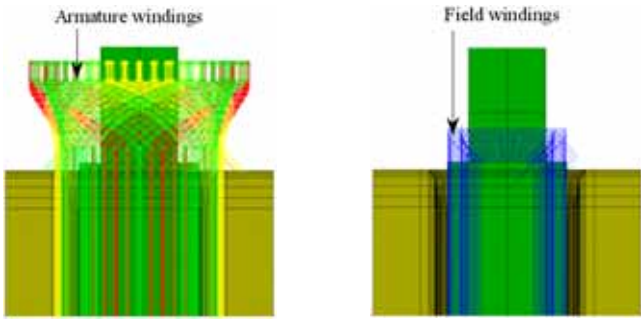

(b) Armature winding (c) Field winding

Fig. 1 3D FEA analysis model

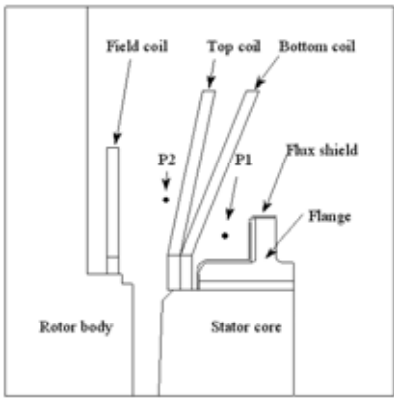

Fig. 2 Axi-periodic analysis model

Analysis result and comparison

Three components of flux densities (B_r, B_θ, B_z) from axi-periodic analysis are compared to those from 3D FEA in Fig. 3, flux densities from axi-periodic analysis agree well with 3D FEA except B_θ at P1. It is expected that the error is caused by the assumption of sinusoidal current distribution in axi-periodic analysis. Therefore, the current distribution in the stator end region is studied.

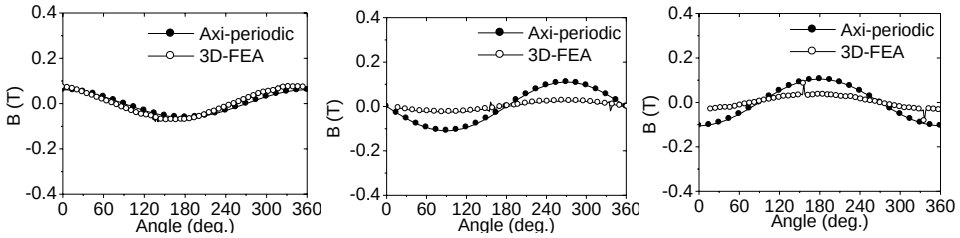

(a) B_r at P1 (b) B_θ at P1 (c) B_z at P1

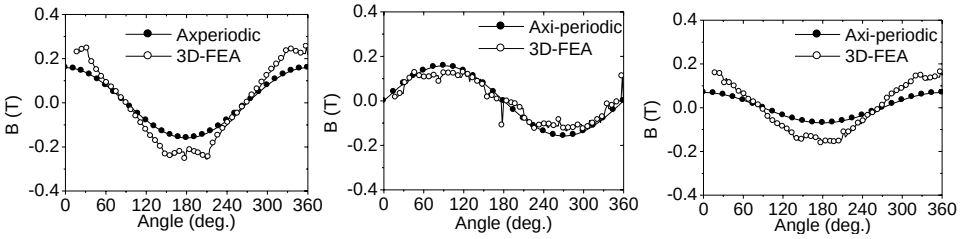

(d) B_r at P2 (e) B_θ at P2 (f) B_z at P2

Fig. 3 Comparison of flux densities from axi-periodic analysis and 3D FEA

Current distribution in end windings

To find out the cause of differences between axi-periodic analysis and 3D FEA, current distribution in the stator end winding according to current phase angle, 3-phase stator end windings is studied. In order to compare the current distributions of axi-periodic analysis model and 3D FEA stator end windings, stator windings are represented as shown in Fig. 4, where solid lines represent coils going out from stator slots, and dot lines represent coil going into stator slots. Coils on the right side of slots are top coil and on the left side are bottom coil. Peak value of 3-phase current is set to 1. When a-phase current is peaking, I_θ, and I_z along line L1 and L2 are calculated and compared to sine and cosine function in Fig.5.

In Fig. 3 (b), the compassion shows a big difference. The difference is caused by the I_z current and this is shown in Fig. 5 (b), where I_z producing B_θ in the 3D FEA model is zero, while that in axi-periodic model has some value.

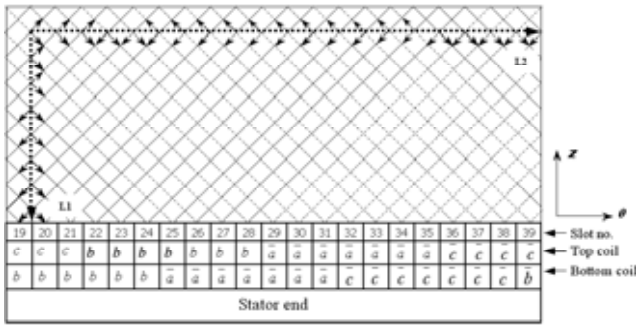

Fig. 4 Current distribution on the stator end winding

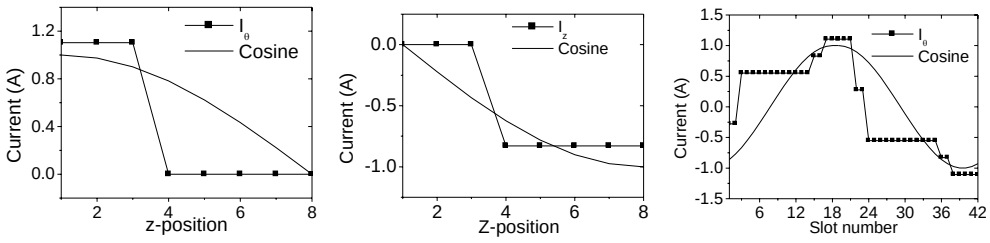

(a) I_θ along L1 (b) I_z along L1 (c) I_θ along L2

Fig. 5 Estimation of current distribution on the stator end windings

APPLICATIONS

Eddy current loss in the flux shield is calculated using (14), where, p_e^k, k, J_e^k, and σ^k are the eddy current loss in flux shield, harmonic order, eddy current density, conductivity in flux shield respectively. Only fundamental component of eddy current density is considered in this paper.

$$p_e^k = \frac{1}{2}\mathrm{Re}\left[\int_v \frac{J_e^k \cdot J_e^{k*}}{\sigma^k}\right] \quad , \; P_e = \sum_k p_e^k \;[\mathrm{W}] \tag{14}$$

In Fig. 6, (a) shows the eddy current loss in the flux shield for power angle. For the leading power angles, field from rotor windings and stator windings are additive, on the contrary, field are subtractive in lagging power angle. Therefore, higher eddy current loss is produced in the leading power angle than lagging power angle.

In Fig. 6, (b) flux distribution due to the eddy current in the flux shield at no load is shown. Because of eddy current in the flux shield, flux caused by end windings tends to take other paths around flux shield. In the figure, four corners in the flux shield show high flux densities, therefore it can be said that the flux density on the surface of flux shield represents the eddy current distributions. Therefore, in the figure, regions of high flux density have high eddy current density, and high temperature is expected.

The effect of flux shield is shown in Fig. 7. When the frequency is 0Hz, that is DC field, flux caused by end windings goes to the stator end directly, therefore, the flux shield does not work. However, when the frequency is 60Hz, eddy current is induced in the flux shield and flux caused by end windings cannot go through stator end directly.

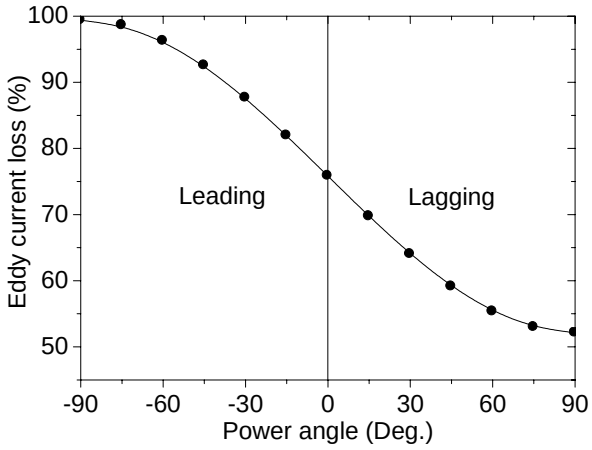

(a) Eddy current loss for load conditions

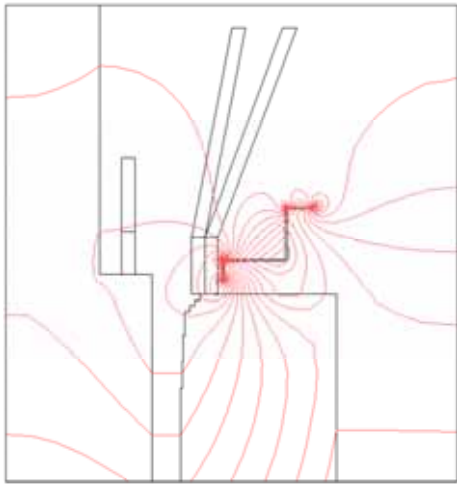

(b) Flux caused by eddy current in the flux shield

Fig. 6 Eddy current loss of the flux shield and flux distribution due to eddy current in flux shield

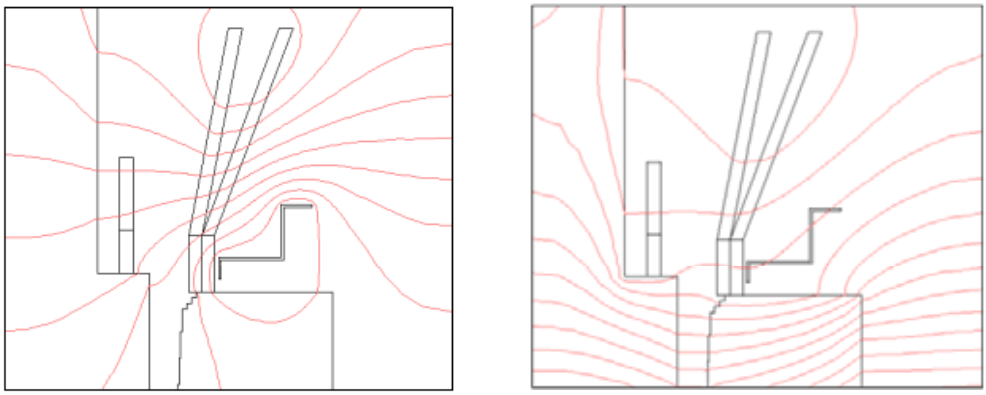

(a) Flux distribution at 60Hz (b) Flux distribution at 0Hz

Fig. 7 Flux distribution for frequencies

Conclusion

Axi-periodic analysis for magnetic field of end region in large turbine generator is studied and verified by 3D FEA in this paper. Due to the differences between the sinusoidal current distribution and the actual one, comparison of flux distribution on the end region shows the differences, and the difference is proved by the comparison of current distribution on the stator endwindings. In spite of the error of axi-periodic analysis, considering the effort and calculation time for 3D FEA, the error would be acceptable for initial design of large turbine generator. For the applications of the axi-periodic analysis, the effect of flux shield on the flux distribution of end region is shown and eddy current loss of flux shield is calculated for power angle, and the application can be extended to the geometry design of flux shield, stepped core, calculation of force in the end windings.

References

[1] G.K.M. Khan, G.W. Buckley, R.B. Bennett, N. Brooks, "An Integrated Approach for the Calculation of Losses and Temperatures in the End-region of Large Turbine Generators", *IEEE Trans. on Energy Conv.,* Vol.5, No. 1, March 1990.

[2] Kaoru Ito, Tadashi Tokumasu, Susumu Nagano, Makoto Tari, Shin-ichi Doi, "SIMULATION FOR DESIGN PURPOSE OF MAGNETIC FIELDS IN TURBINE-DRIVEN GENERATOR END REGION", *Trans. on Power Apparatus and Systems*, Vol. PAS-99, No. 4 July/Aug 1980.

[3] Sheppard J. Salon, "Finite element analysis of electrical machines", Kluwer academic publishers, 1995.

[4] G.K.M Khan, G.W.Buckley, N. Brooks, "Calculation of forces and stresses on generator end–windings- part I: Forces", *IEEE Trans. Energy Conv.,* vol.4, No. 4, December 1989.

[5] V. Varbero, G. Dal Mut, G. Grigoli, M. Santamaria, "Axisymmetric analysis and experimental measurements of magnetic field in the end region of a turbine generator", *IEEE Tran. on Magn.,* vol. MAG-19, no. 6, November, 1983.

[6] Gary Bedrosian, M.V.K. Chan, Manoj Shah, George Theodossiou, "AXIPERIODIC FINITE ELEMENT ANALYSIS OF GENERATOR END REGIONS PART I - THEORY", *IEEE Trans .on Magnetics*, vol. 25, No. 4, July 1989.